SCIENTIFIC REPORTS

OPEN

SUBJECT AREAS:
MEDICAL RESEARCH
PRE-CLINICAL STUDIES

Received
27 February 2014

Accepted
11 June 2014

Published
1 July 2014

Correspondence and requests for materials should be addressed to G.D.L. (gluker@umich.edu)

* These authors contributed equally to this work.

Macroscopic Stiffness of Breast Tumors Predicts Metastasis

Joseph Fenner[1]*, Amanda C. Stacer[1]*, Frank Winterroth[2]*, Timothy D. Johnson[3], Kathryn E. Luker[1] & Gary D. Luker[1,2,4]

[1]University of Michigan Medical School, College of Engineering, and School of Public Health. University of Michigan Center for Molecular Imaging, Department of Radiology, [2]University of Michigan Medical School, College of Engineering, and School of Public Health. University of Michigan Center for Molecular Imaging, Department of Biomedical Engineering, [3]University of Michigan Medical School, College of Engineering, and School of Public Health. University of Michigan Center for Molecular Imaging, Department of Biostatistics, [4]University of Michigan Medical School, College of Engineering, and School of Public Health. University of Michigan Center for Molecular Imaging, Department of Microbiology and Immunology.

Mechanical properties of tumors differ substantially from normal cells and tissues. Changes in stiffness or elasticity regulate pro-metastatic behaviors of cancer cells, but effects have been documented predominantly in isolated cells or *in vitro* cell culture systems. To directly link relative stiffness of tumors to cancer progression, we combined a mouse model of metastatic breast cancer with *ex vivo* measurements of bulk moduli of freshly excised, intact tumors. We found a high, inverse correlation between bulk modulus of resected tumors and subsequent local recurrence and metastasis. More compliant tumors were associated with more frequent, larger local recurrences and more extensive metastases than mice with relatively stiff tumors. We found that collagen content of resected tumors correlated with bulk modulus values. These data establish that relative differences in tumor stiffness correspond with tumor progression and metastasis, supporting further testing and development of tumor compliance as a prognostic biomarker in breast cancer.

For patients with breast cancer and almost all solid malignancies, localized tumors can be treated effectively with surgery and/or radiation therapy, leading to favorable rates of disease-free and overall survival. However, once patients develop clinically detectable metastases, the likelihood for cure drops dramatically with most treatments providing only palliation[1]. To optimize cancer therapy and reduce numbers of patients with progressive disease, there is an ongoing need for prognostic biomarkers that reliably define patients at increased risk of local recurrence or metastatic disease[2]. Patients likely to develop metastases would receive more aggressive neoadjuvant or adjuvant therapies to eliminate disseminated tumor cells and prevent macroscopic metastases. By comparison, patients unlikely to have progressive disease would be treated more conservatively, limiting exposure to toxic drugs. Such an approach based on validated biomarkers is expected to improve outcomes and quality of life for patients with cancer.

Advances in technologies for sequencing DNA and RNA have contributed to a focus on genetic drivers of cancer progression. Indeed, genetic approaches have identified a large number of novel oncogenic fusions, mutations, and gene amplifications in addition to loss of key tumor suppressor genes that appear to be critical for carcinogenesis, metastasis, and disease outcome[3]. For example, the Oncotype DX® 21 gene assay predicts the likelihood of disease recurrence for patients with early stage, estrogen receptor positive breast cancer, which aids selection of patients likely to benefit from endocrine therapy combined with chemotherapy[4]. Only a limited number of genetic abnormalities and signatures have become clinically-used biomarkers for cancer[5]. Given the ongoing challenges of biomarker development, it is essential to broaden the search for prognostic biomarkers to inform decision-making.

The widespread focus on genomic analyses has overshadowed the importance of mechanical and biophysical perturbations in cancer as determinants of disease progression[6]. Deformability is one particularly promising mechanical property for classifying cancer cells. At a single cell level, a variety of different techniques, such as microfluidic devices and atomic force microscopy, typically show that metastatic cancer cells from cell lines and patients are more compliant than non-metastatic cells[7–9]. The ability of metastatic cancer cells to deform is proposed to facilitate migration through extracellular matrix and transit into and out of the vasculature[10]. On a macroscopic scale, malignant tumors typically are characterized as stiffer than normal tissue due in part to contraction of collagen in the extracellular matrix by malignant and stromal cells[11–13]. However, greater

contraction of extracellular matrix and overall stiffness in a tumor do not necessarily correlate with invasiveness of cancer cells in cell culture systems, and few studies have addressed how stiffness of a tumor corresponds with metastasis *in vivo*[14,15].

We used orthotopic implantation of syngeneic mouse breast cancer cells in C57BL/6 mice to investigate a relationship between macroscopic deformation of breast tumors and progression to metastatic disease. We used a piston compression device to measure stiffness of freshly excised mammary tumors, allowing us quantify compliance in intact tumors. Remarkably, we found that mice with the most compliant mammary tumors had significantly more metastases than animals with stiffer tumors, even though mammary tumors did not differ in overall weight or relative numbers of malignant cells. We also demonstrated that overall stiffness of tumors correlated with amount of collagen. These results reveal a high correlation between overall deformation of mammary tumors and progression to metastatic disease. Potentially, this mechanical property of breast tumors may be used to improve identification of patients at increased risk for local recurrence or metastases.

Results

Tumor compliance does not correlate with mass/size of orthotopic tumor implants. To investigate the relationship between mechanical compliance and tumor growth and metastasis, we used a syngeneic C57BL/6 mouse breast cancer cell line (AT-3) originally derived from a breast cancer arising in MMTV-PyMT transgenic mice[16]. We implanted AT-3 cells stably transduced with firefly luciferase (AT-3-FL) and mouse mammary fibroblasts (MMF) expressing chemokine CXCL12 into 4th inguinal mammary fat pads of mice. Co-implanting MMF with AT-3-FL cells reproduces the environment of primary human breast cancers in which carcinoma-associated fibroblasts secrete CXCL12, increasing tumor growth, angiogenesis, and metastasis[17]. In this model, AT-3-FL cells generate mammary tumors that metastasize spontaneously to bone marrow, lung, and other common sites of breast cancer metastases in patients.

We monitored growth of mammary tumors by bioluminescence imaging and palpation. When mammary tumors reached approximately 0.3 g, we resected tumors to mimic treatment of patients with breast cancer for whom surgical removal of a primary tumor is standard therapy. This experimental protocol also eliminates the need to euthanize mice for size of mammary tumors, allowing time for disseminated tumor cells to form macroscopic metastases. Within a cohort of mice, bioluminescence imaging showed comparable photon flux values for tumor implants in all mice, demonstrating that all tumors had similar numbers of viable breast cancer cells (Fig. 1A).

To quantify compliance of freshly resected, unfixed mammary tumors, we used a cylindrical piston compression device based on a system described originally by Erkamp (Fig. 1B)[18,19]. This compression device allows us to indent tumors at precisely determined step increments and determine changes in force for each successive step. Representative stress-strain curves for individual tumors resected from one group of mice are shown in Fig. 1C. For these and other groups of mice, we identified three distinct groups of tumors based on measurements of the bulk modulus from resected tumor implants: 1) tumors with greater stiffness than control values from normal mammary fat pad ("stiff"); 2) tumors with stiffness comparable to normal mammary fat pads ("average"); and 3) tumors that were more compliant than control ("compliant"). Two standard measures of tumor burden, bioluminescence imaging data from the day prior to resection and weight of resected tumors, did not correlate with bulk moduli data for these three groups (Fig. 1D, 1E). Therefore, excised tumors from these groups of mice were comparable except for differences in tumor compliance.

Tumor compliance correlates with tumor recurrence and metastasis. After resection of the initial tumor implant, all mice developed recurrent tumors in the mammary fat pad and systemic metastases. Bioluminescence imaging data from the day prior to euthanization, which is dominated by recurrent tumor in mammary fat pads, showed a high correlation between photon flux for AT-3-FL cells and bulk modulus data for resected tumors (Fig. 2A, B). Mice with the most compliant resected tumors had the highest values for photon flux, while stiffer tumors correlated with lower burden of breast cancer cells ($p < 0.001$). Data for bulk moduli of tumors at the time of initial resection also corresponded with rank order of weights of recurrent mammary tumors, even though weights of initially resected tumors did not correlate with measurements of bulk moduli (Fig. 2C). In addition, the mechanical properties of mammary tumors generally remained consistent over time. Stiffer resected tumors gave rise to stiffer recurrent tumors, while more compliant tumor implants produced relatively more compliant recurrent tumors in the mammary fat pad.

We also analyzed overall and site-specific metastases relative to differences in compliance of tumor implants. Dark fur and pigmentation of C57BL/6 mice scatter and attenuate light, which may obscure bioluminescence from small metastases. Therefore, we imaged bioluminescence in minimally dissected mice immediately after euthanization to improve sensitivity for metastatic foci[20]. Mice with stiff mammary tumors as quantified by our piston compression method had minimal metastases relative to mice with the most compliant tumors (Fig. 3A). Bioluminescence imaging showed a rank order of overall metastases of stiff $<$ average $<$ compliant bulk moduli from mammary tumors (Fig. 3B). Differences for metastases from compliant tumors versus other groups were of borderline significance ($p = 0.057$). Compliant tumors produced more metastases in multiple anatomic sites, including chest, abdomen, omentum, and bone marrow (Fig. 3C). Most notably, the bulk modulus of a mammary tumor in each mouse correlated inversely with metastases with more compliant mammary tumors producing greater metastases and vice versa (Fig. 3D) ($p = 0.0004$).

Collagen content in tumors correlates with macroscopic tumor compliance. Collagen is the major structural component of the extracellular matrix in breast cancers, suggesting that collagen content may determine bulk compression properties of mammary tumors in our mouse model. We stained paraffin sections of mammary tumor implants with Masson's trichrome to detect collagen. Representative images qualitatively show a range of collagen content in tumors, encompassing tumors with minimal collagen (Fig. 4A) to progressively greater amounts of this extracellular matrix molecule. We quantified amounts of collagen in tumor sections by ImageJ, normalizing the area occupied by collagen to the area of each view field comprised of cells. This analysis revealed a significant direct correlation between collagen content in each tumor and its bulk modulus value from compression studies with higher amounts of collagen corresponding with greater values for bulk moduli (Fig. 4B). By comparison, all tumors showed comparable overall architecture and cellularity by H&E staining (Fig. 4C). Overall, these data establish collagen as a key feature that determines macroscopic deformation of mammary tumors.

Discussion

Ongoing studies emphasize that behaviors of cancer cells, including signaling, invasion, and proliferation, depend on biomechanical properties of individual cells and the extracellular matrix environment[21,22]. Both metastatic cancer cell lines and primary cancer cells recovered from metastatic sites typically show greater deformability than non-metastatic counterparts in a variety of *in vitro* assays[23,24]. Changes in stiffness of the extracellular matrix regulate expression of pro-metastatic genes and also may correlate with progression from

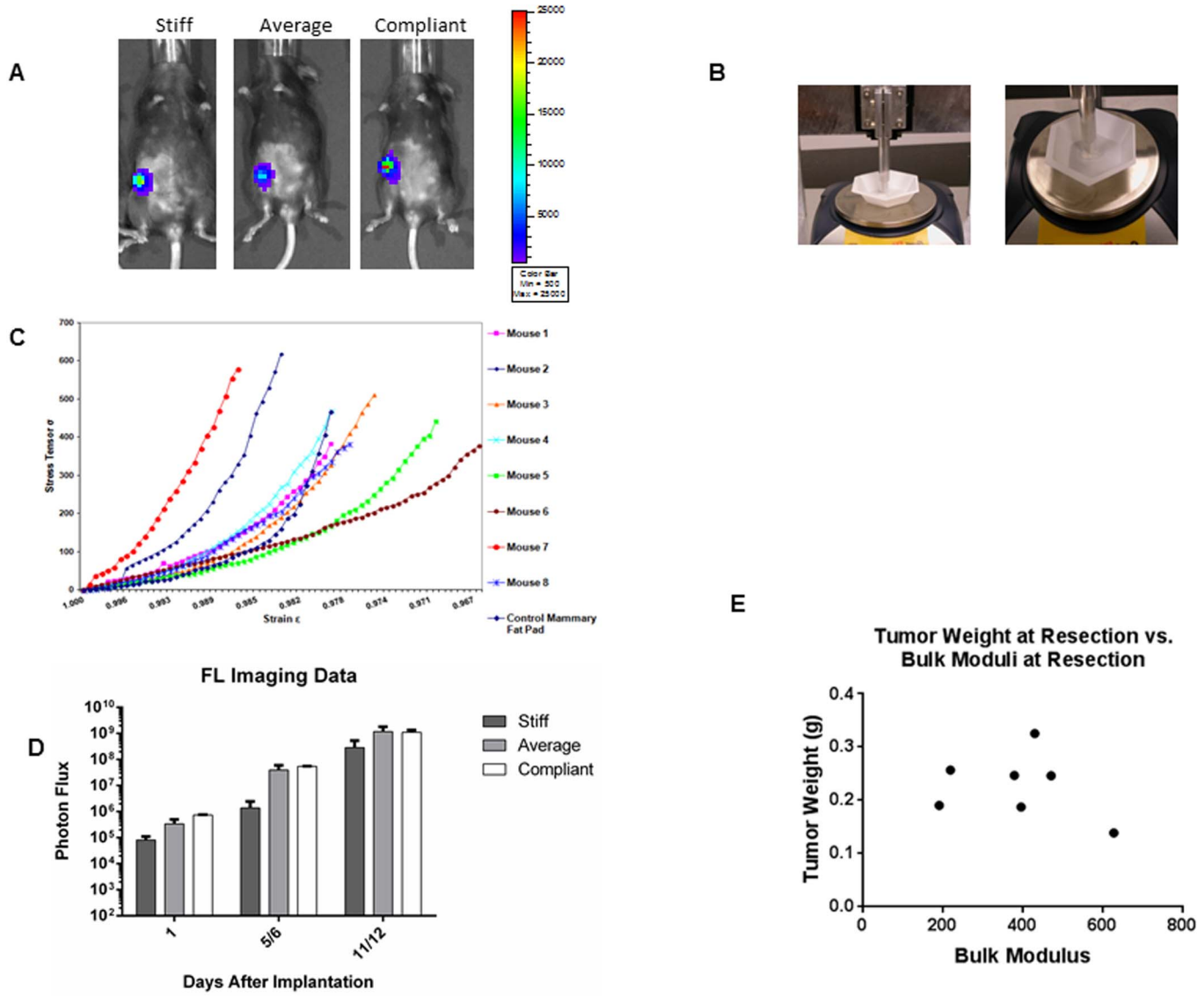

Figure 1 | Bulk modulus measurements separate mammary tumors into distinct groups of compliance. (A) Representative bioluminescence images of mice with orthotopic mammary tumor implants of AT-3-FL breast cancer cells. Images are from mice with relatively compliant (left) or stiff tumors at the time of resection. (B) Photo of piston compression device system used to measure bulk moduli of tumors *ex vivo*. We position the cylindrical piston over a tumor in a weigh boat on top of a tared digital scale. The piston applies vertical compression perpendicular to the surface of the tumor. (C) Graph depicts representative strain versus stress values for freshly excised tumor implants. Each curve is from a single mouse. Brackets group curves into tumors with lower, comparable, or higher compliance than control mammary fat pads, designated as stiff, average, and compliant, respectively. (D) Graph displays correlation coefficients from strain-stress data versus photon flux values from bioluminescence imaging for individual tumors. Imaging data are from the day prior to resection of the tumor implant. (E) Graph of correlation coefficients from strain-stress data of resected tumor implants versus tumor weight.

normal epithelium to malignancy[25–28]. However, biomechanical studies of cancer typically rely on invasion assays or other surrogate, *in vitro* behaviors of malignancy to correlate with cellular and extracellular stiffness. As a result, it remains difficult to directly relate biomechanical properties of cancer to relevant endpoints of tumor progression in living subjects.

We employed a cylindrical piston compression device to analyze macroscopic compression of freshly resected, intact mammary tumors *ex vivo*. Nonlinear elastic properties of different soft tissues and certain commercially available graft materials previously have been determined using a Fung strain energy function[29], but no similar studies have applied to malignant tumors. The piston compression device probes perpendicular to layers of cells in tumors. Under this condition, individual tumors simplistically behave similar to springs in series. The reciprocal of the constituent spring constants average, so softer materials, such as more compliant cancer cells, dominate the measurement. Tissue elasticity is a more complicated function of elastic coefficients from components including different types and amounts of cells, extracellular matrix, and fat. As shown histologically, implantable tumor models used in this study show only modest differences among cell types, relative overall cellularity, and fat content in comparison to variability in human breast cancers. In the context of future studies with human tumors, we may need to utilize high-frequency (50–60 MHz) ultrasound coupled with compression methods to quantify degrees of stress-strain deformations at specific locations within a tumor. This approach potentially will allow us to determine specific components of a tumor that contribute to defined stages of deformation relative to strain.

We combined the piston compression measurement technique with a mouse model of breast cancer that reproduces surgical

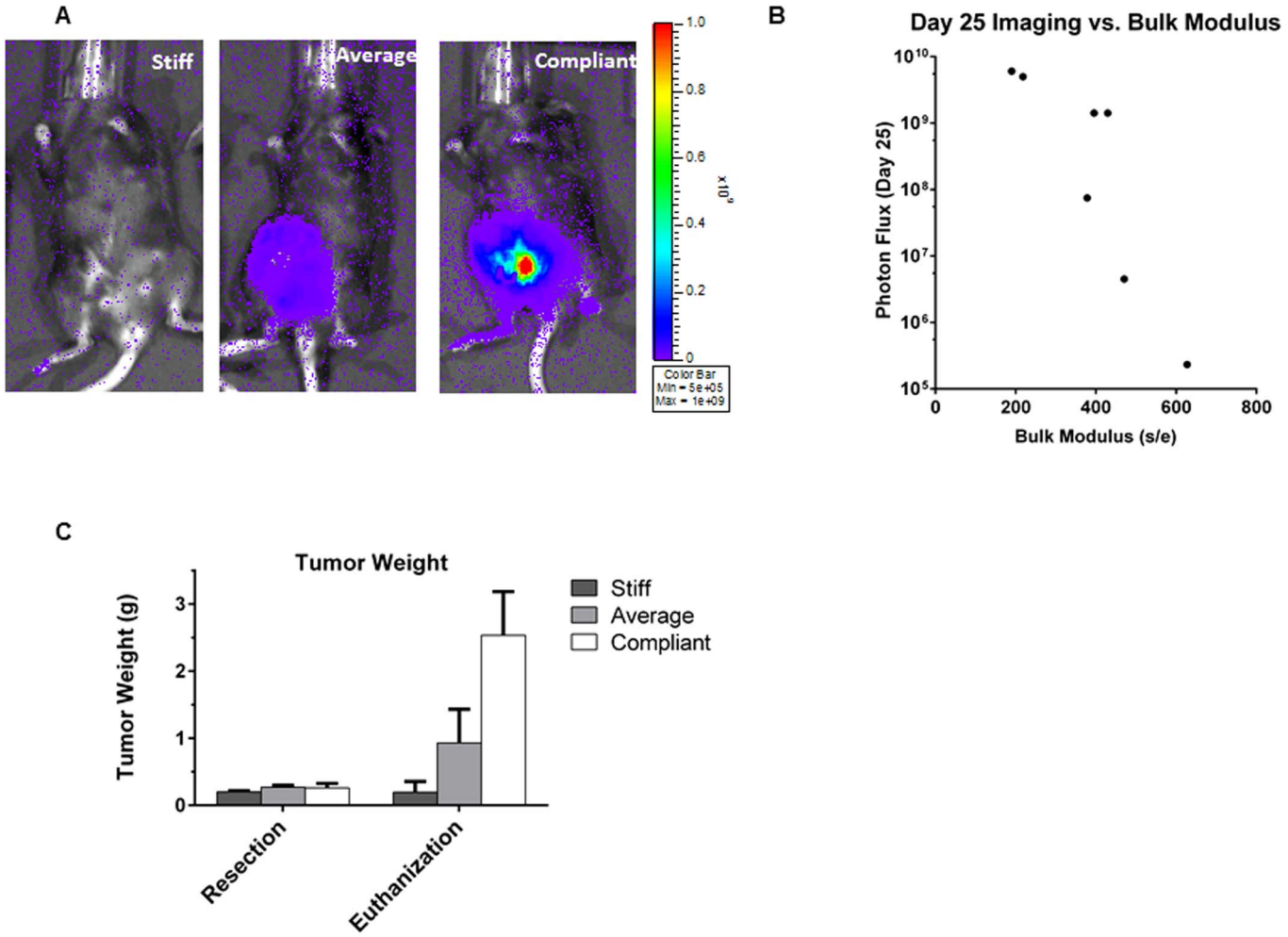

Figure 2 | Mice with compliant tumors at initial resection have larger local recurrent tumors. (A) Representative bioluminescence images of recurrent tumors in mammary fat pads of mice with stiff, average, or compliant mammary tumors at the time of initial resection. (B) Graph of bulk modulus for resected tumors and photon flux for recurrent tumors in the mammary fat pad. Each data point represents an individual mouse. Bulk modulus and photon flux values are correlated inversely ($p < 0.005$).

resection of a mammary tumor with subsequent local recurrence and metastasis. Using this approach, we established that tumors with greater macroscopic compliance were more likely to recur at the surgical site and metastasize to multiple anatomic sites. Differences in disease progression based on mechanical compliance were independent of tumor weight and numbers of viable tumor cells measured by bioluminescence imaging. Furthermore, tumors generally retained biomechanical properties during tumor progression with more compliant mammary tumors at the time of initial resection remaining comparatively more compliant at local recurrence. Relative stability of tumor compliance over time suggests that at least part of tumor compliance is maintained through genetic and/or epigenetic changes in malignant cells[30]. Overall, these results suggest that greater compliance facilitates invasion, vascular intravasation, and extravasation of malignant cells, which are processes that promote local recurrence and distant metastases as we observed.

Studies of biomechanics in cancer typically have been performed with isolated malignant cells or cell culture systems because of the methods used to test and experimentally manipulate stiffness. A variety of experimental methods have shown that individual metastatic cancer cells are notably more compliant and deformable than non-metastatic cancer cells or matched normal epithelium[31–33]. However, cancer cells exhibit variable responses to stiffer matrices. In a three-dimensional cell culture model of neuroblastoma, increasing stiffness of the type I collagen extracellular matrix caused malignant cells to differentiate and become less invasive[25]. Two-dimensional cultures of hepatocellular carcinoma cells proliferated more rapidly on stiffer gels, but relatively softer surfaces enriched for quiescent cells with properties of tumor initiating cells[34]. Similarly, culturing cancer cells on soft fibrin gels promotes growth of cells with enhanced tumor initiating capability as compared with stiffer matrices[35]. Potentially, more compliant tumors were enriched for tumor initiating cells in our study, accounting for greater local recurrence and metastases.

Both studies of isolated cells and three-dimensional cell cultures inherently lose overall effects of tumor architecture and possible effects of the tumor environment and signaling milieu on mechanical properties. A prior study mapping tumor elasticity *in situ* showed substantial regional heterogeneity in stiffness, highlighting the importance of analyzing mechanical properties of tumors under conditions that maintain native architecture[36]. While the piston compression method is limited to quantifying overall elasticity of a tumor, this method enables efficient processing of multiple fresh tumors and direct comparison of deformability to subsequent outcomes.

Effects of collagen, the primary component of extracellular matrix in breast tissue, on breast cancer incidence and progression have been studied extensively. Patients with dense breasts on mammograms, an x-ray based imaging technique used for breast cancer screening, have a significantly greater risk of breast cancer than

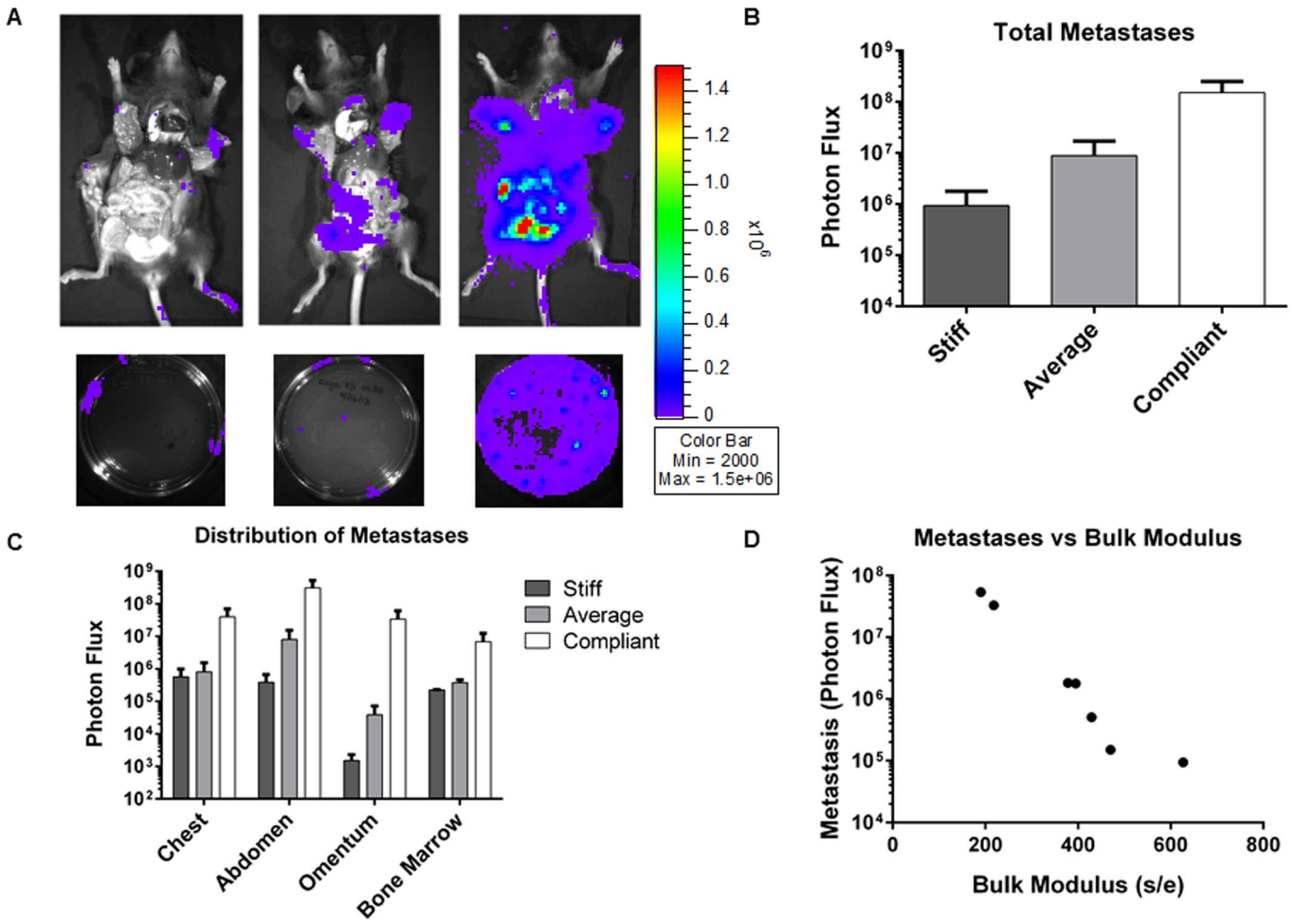

Figure 3 | Compliant tumors correlate with greater metastases. (A) Representative bioluminescence images of metastases in mice with stiff, average, and compliant tumors. All images are shown on the same pseudocolor scale depicted by the scale bar. Images of plates show representative bone marrow metastases recovered from the same three groups of mice based on bulk moduli. (B) Graph shows mean values + SEM for total metastases in mice with stiff, average, and compliant tumors at time of resection (n = 4–6 per group). (C) Graph of mean values + SEM for photon flux from metastases to specific anatomic sites. (D) Graph shows data points for bulk modulus versus photon flux values for metastases from individual mice. There is a significant inverse correlation between bulk modulus of a resected tumor and subsequent development of metastases ($p < 0.0004$).

women with predominantly fatty breast tissue[37]. Despite a well-documented association with cancer incidence, effects of collagen content on outcomes of breast cancer remain uncertain. In a mouse model of breast cancer, Levental et al experimentally increased cross-linking, but not overall content, of collagen in mammary tissue, which augmented invasion of malignant cells into normal breast stroma[26]. Studies in patients using two-photon laser excitation with second harmonic imaging or mammographic density to assess collagen content in breast cancers frequently show an increased risk of regional lymph node metastasis with greater amounts of collagen[38,39]. However, the direct correlation between collagen and lymph node metastases in breast cancer is not consistent across all studies with some data suggesting an inverse relationship[40]. Amounts of collagen in breast tissue are not clearly related to outcome in patients with breast cancer; the largest study failed to identify a relationship between mammographic density and death[41]. Our study found that amounts of collagen identified histologically corresponded with overall stiffness of tumors, but stiffer tumors had fewer metastases. These discordances among studies emphasize complexities of relating perturbations in the extracellular matrix to outcomes in breast cancer and other malignancies and suggest that other cellular and/or extracellular parameters contribute to the impact of biomechanics on tumor biology.

Overall, our data indicate that macroscopic measurements of tumor compliance in breast cancer may identify tumors with increased probability of local recurrence and metastasis. The correlation of tumor compliance with metastasis may reflect that specific signaling pathways in cancer dictate biomechanics of malignant cells and extracellular matrix, and physical properties of the environment can control oncogenic signaling. Elucidating molecules and signaling pathways that link genetics and mechanics of cancer likely will reveal new targets and approaches to improve therapy. Further studies of elasticity in intact tumors, using *in vivo* imaging techniques such as ultrasound or magnetic resonance elastography or *ex vivo* mechanical compression devices such as used in this paper, are warranted to determine the value of tumor compliance as a prognostic marker in patients[42,43]. While tumor compliance may not be sufficiently accurate to become a stand-alone prognostic biomarker, we envision that adding this parameter to other molecular and clinical data will improve identification of patients at increased risk for local recurrence or metastases.

Experimental

Cells. We used AT-3 and E0771 mouse breast cancer cells (gifts of Dr. Abrams and Dr. Mihich, respectively, from Roswell Park Cancer Institute) and immortalized mouse mammary fibroblasts (gift of Dr.

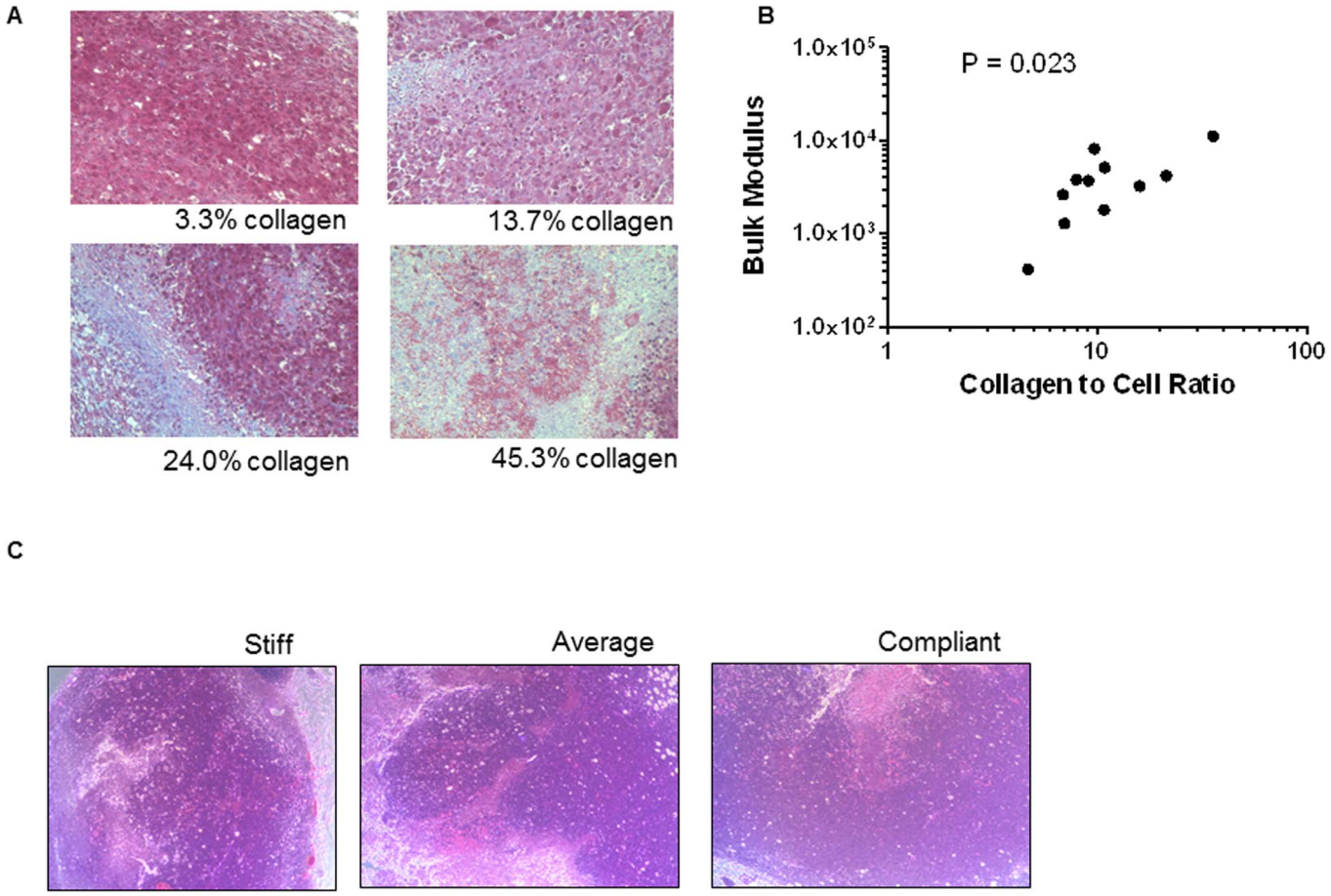

Figure 4 | Collagen content of tumors corresponds with macroscopic bulk moduli of tumors. (A) Masson's trichrome staining of resected tumor implants shows collagen in blue-purple. Values listed in each image are the percent area occupied by collagen relative to cells in each field. (B) Graph shows a significant correlation between normalized area of each image occupied by collagen versus bulk modulus for individual tumors ($p = 0.023$). Each data point represents a different tumor. (C) Representative H&E stained histologic sections from tumors measured as stiff, average, or compliant.

Moses, Vanderbilt University). AT-3 adenocarcinoma cells lack estrogen and progesterone receptors; these cells also do not over-express Her2, which classifies the cells as "triple negative". E0771 cells are an estrogen-receptor positive medullary adenocarcinoma. We cultured all cells in DMEM (Life Technologies) supplemented with 10% fetal bovine serum and 1% glutamine/penicillin/streptomycin (Life Technologies). We maintained all cells in a 37°C incubator with 5% CO_2.

Lentiviruses. We transduced breast cancer cells with a lentiviral vector for firefly luciferase, generating AT-3-FL and E0771-FL cells, respectively, for bioluminescence imaging[44]. E0771 cells also stably expressed unfused green fluorescent protein (E0771-FL-GFP). To reproduce secretion of chemokine CXCL12 by stromal fibroblasts in breast cancer, we stably transduced mouse mammary fibroblasts with CXCL12 fused to fluorescent protein mCherry (MMF-CXCL12)[17,45].

Animal studies and imaging. All animal procedures were approved by the University of Michigan Committee for the Use and Care of animals and performed in accordance to the protocol. To establish orthotopic breast tumors, we injected 1×10^5 MMF-CXCL12 cells with either 2×10^5 AT-3 –FL or 2×10^5 EO771-FL-GFP cells into the 4th inguinal mammary fat pads of 6-7 week old female C57BL/6 mice. When tumors grew to approximately 0.3 g, we resected tumors to allow time for mice to develop metastases detectable by bioluminescence imaging[44]. We quantified tumor growth and metastasis based on photon flux values from bioluminescence imaging[46]. When mice had to be euthanized because of tumor burden, we imaged metastasis in minimally dissected mice as described previously[20].

Compression studies. We resected tumors from mice and stored them in PBS on ice until performing compression studies within 30–45 minutes. We used normal mammary fat pads from mice without tumors as a control. The tumor compression set-up is derived from the experiments originally performed by Erkamp, in which a cylindrical sample was indented while mounted on top of a weigh boat[18,19]. The system to measure the nonlinear elastic behavior of soft tissue is an in-house built compressor using a cylindrical piston of known length and volume to indent the tumor sample at steps of a known length, registering as a change in mass (in grams) on an electronic scale (Ohaus Scout Pro SPE602, Pine Brook, NJ. USA.) tared to the weight of the specimen, and recording changes in force for each successive step size (10 μm) that the cylindrical piston was applied to the specimen; this compressor set up is illustrated in Figure 1B. The piston is mounted directly over the center of the tumor and pushes on it, producing a known amount of force. This force, plus knowing the degree of surface displacement, provides the nonlinear geometric stiffness characteristic for the given tumors. The equipment is a simpler version of the setup used to measure nonlinear elastic properties[18,19]. All stress levels were measured as Pascals in relation to strain levels of known compression step length. Gram to Newton force conversion was applied to obtain the appropriate force for each step using the following equation:

$$\mathbf{F} = [(\mathbf{gr}/\mathbf{1000}) * \mathbf{9.80665}] \quad (1)$$

where gr is the piston load in grams registered by the scale. For nonlinear elastic analysis, we measured the compressive stress and deformation.

The stress measure is the 1st Piola-Kirchoff stress T defined as the current measured force divided by the original specimen area A:

$$\mathbf{T} = \mathbf{F}/\mathbf{A}' \quad (2)$$

where the current force F is defined by equation 1 and A' is the area of a tumor specimen before deformation. The stretch ratio l is simply defined as the deformed height of the specimen l divided by the original height of the specimen (l_0 as $\lambda = l/l_0$). We further assume that the tumor is incompressible (i.e. its volume does not change during deformation). Since the deformation gradient tensor F_{ij} only has diagonal stretch ratios λ_1, λ_2, and λ_3 under the applied deformation, this implies that $l_1 l_2 l_3 = 1$. The deformation is applied in the vertical (l_3) direction, and we further assume that the stretch ratios in the l_2 and l_3 direction are equal and due to incompressibility are related to l_3 by:

$$\boldsymbol{\lambda_1} = \sqrt{\frac{\mathbf{1}}{\boldsymbol{\lambda_3}}} \quad (3)$$

Histology. We fixed tumors in a 10% formalin solution overnight. Tumors then were embedded in paraffin blocks for sectioning by the Unit for Laboratory Animal Medicine Pathology Cores for Animal Research (PCAR) at the University of Michigan. PCAR also stained sections with hematoxylin and eosin (H&E) for general histology or Masson's trichrome to delineate collagen. We took images of tissue sections at 20× magnification on an Olympus IX70 microscope using Spot Advanced Software (Spot Imaging).

Image Quantification. We used ImageJ to quantify collagen content in tumors (nine images per tumor with three images per separate section). The method utilized was adapted from a method on the NIH website used to quantify stained liver tissue (see http://rsbweb.nih.gov/ij/docs/examples/stained-sections/index.html). Each image was converted from a RGB color image to a RGB stack (grayscale) and analyzed in the green channel. We noted three areas of interest within the grayscale image: a dark gray region representative of stained cytosol (pink in color image), a significantly lighter gray region representative of the stained collagen (blue in color image), and a white region indicative of dead space within in the tumor. The green channel provided the best separation of these regions to isolate collagen. We manually set a threshold for each image using the over/under threshold feature, which allowed us to eliminate pixels darker (cellular cytosol) and lighter (dead space) than pixels representative of collagen. Upper threshold values were set at approximately 210, while lower threshold values ranged around 170. The thresholded images were then compared alongside original images to validate the approximate 170–210 range chosen for collagen. Each image was measured for percent area occupied by collagen, resulting in 9 measurements per tumor.

Statistical analysis. To determine root mean square (RMS) values for nonlinear elastic properties of individual tumors, we used both one-way analyses of variance (ANOVA) and linear regression analyses. Mean collagen values from tumor sections stained with Masson's trichrome stain were plotted alongside mean bulk moduli. We determined the correlation between these parameters with a nonparametric Spearman rank correlation test because the data sets were far from the bivariate normal. We analyzed other pairs of data by unpaired T test to determine statistically significant differences ($p < 0.05$) (GraphPad, Prism).

1. Metastatic Cancer. *United States National Cancer Institute* http://www.cancer.gov/cancertopics/factsheet/Sites-Types/metastatic, Reviewed 3/28/2013, accessed 5/7/2014 (2013).
2. Brooks, J. Translational genomics: the challenge of developing cancer biomarkers. *Genome Res* **22**, 183–187 (2012).
3. Vogelstein, B. *et al.* Cancer genome landscapes. *Science* **339**, 1546–1558 (2013).
4. Carlson, J. & Roth, J. The impact of the Oncotype Dx breast cancer assay in clinical practice: a systematic review and meta-analysis. *Breast Cancer Res Treat* **141**, 13–22 (2013).
5. Hayes, D. An audience with Daniel Hayes. *Nat Rev Drug Discov* **12**, 734–735 (2013).
6. Suresh, S. Biomechanics and biophysics of cancer cells. *Acta Biomater* **3**, 413–438 (2007).
7. Cross, S., Jin, Y., Rao, J. & Gimzewski, J. Nanomechanical analysis of cells from cancer patients. *Nat Nanotechnol* **2**, 780–783 (2007).
8. Byun, S. *et al.* Characterizing deformability and surface friction of cancer cells. *Proc Natl Acad Sci USA* **110**, 7580–7585 (2013).
9. Swaminathan, V. *et al.* Mechanical stiffness grades metastatic potential in patient tumor cells and in cancer cell lines. *Cancer Res* **71**, 5075–5080 (2011).
10. Wirtz, D., Konstantopoulos, K. & Searson, P. The physics of cancer: the role of physical interactions and mechanical forces in metastasis. *Nat Rev Cancer* **11**, 512–522 (2011).
11. Butcher, D., Alliston, T. & Weaver, V. A tense situation: forcing tumour progression. *Nat Rev Cancer* **9**, 108–122 (2009).
12. Lu, P., Weaver, V. & Werb, Z. The extracellular matrix: A dynamic niche in cancer progression. *J Cell Biol* **196**, 395–406 (2012).
13. Cox, T. & Erler, J. Remodeling and homeostasis of the extracellular matrix: implications for fibrotic diseases and cancer. *Dis Model Mech* **4**, 165–178 (2011).
14. Zaman, M. *et al.* Migration of tumor cells in 3D matrices is governed by matrix stiffness along with cell-matrix adhesion and proteolysis. *Proc Natl Acad Sci USA* **103**, 10889–10894 (2006).
15. Gilkes, D. *et al.* Collagen prolyl hydroxylases are essential for breast cancer metastasis. *Cancer Res* **73**, 3285–3296 (2013).
16. Stewart, T. & Abrams, S. Altered immune function during long-term host–tumor interactions can be modulated to retard autochthonous neoplastic growth. *J Immunol* **179**, 2851–2859 (2007).
17. Orimo, A. *et al.* Stromal fibroblasts present in invasive human breast carcinomas promote tumor growth and angiogenesis through elevated SDF-1/CXCL12 secretion. *Cell* **121**, 335–348 (2005).
18. Erkamp, R., Wiggins, P., Skovoroda, A., Emalianov, S. & O'Donnell, M. Gold standard system for reconstructive elasticity imaging. *Ultrason Imaging* **19**, 60–61 (1997).
19. Erkamp, R., Wiggins, P., Skovoroda, A., Emalianov, S. & O'Donnell, M. Measuring the elastic modulus of small tissue samples. *Ultrason Imaging* **20**, 17–28 (1998).
20. Luker, K. *et al.* Scavenging of CXCL12 by CXCR7 Regulates Tumor Growth and Metastasis of CXCR4-positive Breast Cancer Cells. *Oncogene* **31**, 4570–4578 (2012).
21. Kumar, S. & Weaver, V. Mechanics, malignancy, and metastasis: the force journey of a tumor cell. *Cancer Metastasis Rev* **28**, 113–127 (2009).
22. Coughlin, M. *et al.* Cytoskeletal stiffness, friction, and fluidity of cancer cell lines with different metastatic potential. *Clin Exp Metastasis* **30**, 237–250 (2013).
23. Xu, W., Mezencev, R., Wang, K., McDonald, J. & Sulchek, T. Cell Stiffness Is a Biomarker of the Metastatic Potential of Ovarian Cancer Cells. *PLoS One* **7**, e46609 (2012).
24. Cross, S. *et al.* AFM-based analysis of human metastatic cancer cells. *Nanotechnology* **19**, 384003 (2008).
25. Lam, W. *et al.* Extracellular matrix rigidity modulates neuroblastoma cell differentiation and N-myc expression. *Mol Cancer* **10**, 35 (2010).
26. Levental, K. *et al.* Matrix crosslinking forces tumor progression by enhancing integrin signaling. *Cell* **139**, 891–906 (2009).
27. Calvo, F. *et al.* Mechanotransduction and YAP-dependent matrix remodelling is required for the generation and maintenance of cancer-associated fibroblasts. *Nat Cell Biol* **15**, 637–646 (2013).
28. Barcus, C., Keely, P., Eliceiri, K. & Schuler, L. Stiff collagen matrices increase tumorigenic prolactin signaling in breast cancer cells. *J Biol Chem* **288**, 12722–12732 (2013).
29. Yoder, J. & Elliott, D. Nonlinear and anisotropic tensile properties of graft materials used in soft tissue applications. *Clin Biomech (Bristol, Avon)* **25**, 378–382 (2010).
30. Hongmei, Y., Mouw, J. & Weaver, V. Forcing form and function: biomechanical regulation of tumor evolution. *Trends Cell Biol* **21**, 47–56 (2011).
31. Furhmann, A. *et al.* AFM stiffness nanotomography of normal, metaplastic and dysplastic human esophageal cells. *Phys Biol* **8**, 015007 (2011).
32. Zhang, W. *et al.* Microfluidics separation reveals the stem-cell-like deformability of tumor-initiating cells. *Proc Natl Acad Sci USA* **109**, 18707–18712 (2012).
33. Wang, G. *et al.* Stiffness dependent separation of cells in a microfluidic device. *PLoS One* **8**, e75901 (2013).

34. Schrader, J. *et al*. Matrix stiffness modulates proliferation, chemotherapeutic response, and dormancy in hepatocellular carcinoma cells. *Hepatology* **53**, 1192–1205 (2011).
35. Liu, J. *et al*. Soft fibrin gels promote selection and growth of tumorigenic cells. *Nat Mater* **11**, 734–741 (2012).
36. Lopez, J., Kang, I., You, W.-K., McDonald, D. & Weaver, V. *In situ* force mapping of mammary gland transformation. *Integr Biol* **3**, 910–921 (2011).
37. McCormack, V. & dos Santos Silva, I. Breast density and parenchymal patterns as markers of breast cancer risk: a meta-analysis. *Cancer Epidemiol Biomarkers Prev* **15**, 1159–1169 (2006).
38. Kakkad, S. *et al*. Collagen I fiber density increases in lymph node positive breast cancers: pilot study. *J Biomed Opt* **17**, 116017 (2012).
39. Eriksson, L., Czene, K., Rosenberg, L., Humphreys, K. & Hall, P. Possible influence of mammographic density on local and locoregional recurrence of breast cancer. *Breast Cancer Res* **15**, R56 (2013).
40. Wasuthit, Y., Kongdan, Y., Suvikapakornkul, R., Lertsithichai, P. & Chirappapha, P. Predictive factors of axillary lymph node metastasis in breast cancer. *J Med Assoc Thai* **94**, 65–70 (2011).
41. Gierach, G. *et al*. Relationship between mammographic density and breast cancer death in the Breast Cancer Surveillance Consortium. *J Natl Cancer Inst* **104**, 1218–1227 (2012).
42. Sinkus, R. *et al*. High-resolution tensor MR elastography for breast tumour detection. *Phys Med Biol* **45**, 1649–1664 (2000).
43. Evans, A. *et al*. Invasive breast cancer: relationship between shear-wave elastographic findings and histologic prognostic factors. *Radiology* **263**, 673–677 (2012).
44. Smith, M. *et al*. CXCR4 regulates growth of both primary and metastatic breast cancer. *Cancer Res* **64**, 8604–8612 (2004).
45. Ray, P. *et al*. Carboxy-terminus of CXCR7 regulates receptor localization and function. *Int J Biochem Cell Biol* **44**, 669–678 (2012).
46. Luker, G., Pica, C., Song, J., Luker, K. & Piwnica-Worms, D. Imaging 26S proteasome activity and inhibition in living mice. *Nat Med* **9**, 969–973 (2003).

Acknowledgments

Research was supported by grants from the United States Institute of Health R01CA170198, R01CA136553, R01CA142750, and P50CA093990.

Author contributions

J.F., A.C.S., and F.W. performed experiments. K.L. provided new reagents. J.F., A.C.S., and F.W., T.D.J., and G.D.L. analyzed data. J.F., A.C.S., and F.W., and G.D.L. wrote the paper. All authors reviewed the manuscript and approved of submission.

Additional information

Competing financial interests: The authors declare no competing financial interests.

How to cite this article: Fenner, J. *et al*. Macroscopic Stiffness of Breast Tumors Predicts Metastasis. *Sci. Rep.* **4**, 5512; DOI:10.1038/srep05512 (2014).